Experimental study to transport droplets by electrostatic actuation

Joana Ramos[1,2]
[1]IN+, Center for Innovation, Technology and Policy Research, Dep. Mechanical Engineering, Instituto Superior Técnico, Universidade de Lisboa, Portugal
[2]IBB, Institute for Biotechnology and Bioengineering, Center for Biological and Chemical Engineering, Dep. Bioengineering, Instituto Superior Técnico, Universidade de Lisboa, Portugal
*Corresponding author: joana.ramos@ist.utl.pt

Abstract

This study aims at characterizing the dynamic behaviour of droplets of biofluids over enhanced surfaces with and without electrostatic actuation. The best performing enhanced surfaces are chosen based on the characterization of the wettability, quantified by the static contact angle and on the analysis of the temporal evolution of the diameter of the droplets during spreading, which is forced by droplet impact at small velocities. The tests consider the use of 2-3μL droplets of sodium chloride (NaCl), the protein BSA - bovine serum albumin and blood plasma mock (100mM NaCl, 1.2mM BSA, 5.6mM glucose) solutions with different concentrations. The pH of the solutions was also varied. The results show a mild promotion of droplet motion by electrowetting when the concentration of the studied solutes (NaCl, BSA, glucose) was slightly increased. The apparent high saturation observed in the static angles measured on the electowetting tests of BSA solutions, which might cause a limitation in their transportation and handling, is suggested to be caused by the adsorption of this protein on the dielectric substrate, which induces modifications of the local wettability if the droplet stays in contact with the substrate for sufficient time. Analysis of the absorption spectra, before and after electrowetting reveals that BSA remains unchanged after electrostatic actuation, but that the droplet partially evaporates, causing an increase on the concentration of BSA.

Key-words: Electrowetting, biofluids, wettability, BSA, superhydrophobicity, Teflon and microdroplets.

Introduction

Droplet-based transport phenomena driven by surface tension have been explored as an automated pumping source for various chemical and biological applications. Recently, researchers (e.g. [1]) have suggested an alternative microfluidic approach to create fluidic pathways using hydrophobic or superhydrophobic patterns in an open surface configuration, referred to as surface microfluidics. Indeed, control of the fluid motion at the microscale via tailoring of surface tension is advantageous, as it avoids many eletromechanical parts, given that within this scale, surface tension forces become dominant over pressure and body forces. Local modification of the surface tension can be then obtained by a variety of methods, such as electrostatic actuation. This method is actually considered as the backbone of digital microfluidics [2] and many authors point out its potential for transport and manipulation of biological fluids. Some of these applications include DNA and protein analysis as well as biomedical diagnostics (*e.g.* [3-4]). Digital microfluidics for cell assays is also argued to be advantageous when compared to the currently used techniques [5-6]. However, most of the devices developed so far are based on continuous flow through closed channels [7]. Such closed configuration is the easiest to implement, but has several limitations associated to clogging and cleaning issues and difficulties in having access to the samples. The alternative is a single plate open configuration system [8], which brings many challenges in terms of the arrangement of the chip. Here, surface modification has a vital role, but also introduces additional complexity to the system, as the study of the wettability and electrowetting over micro and nanostructured surfaces often cause asymmetries in droplet shape, due to hysteresis [9] and particular droplet morphologies which may not be stable [7]. Hence, although this open configuration has great potential for bioengineering and biomedical applications, as recently reviewed in [10], much research is still required for the production of commercially viable systems. The traditional concept of EWOD – electrowetting on dielectric, stands on the reduction of the dielectric-liquid interfacial energy by

the application of a voltage between a conducting droplet and an underlying dielectric layer. The dielectric layer was introduced by Berge [11], simply to avoid the problem of water electrolysis, which occurs at just a few hundred millivolts. Contrasting to the most current models, which consider the decrease of the contact angle as the governing effect of electrowetting controlled droplet motion, electromechanical [9,12] and energy minimization models [7,13] show that the energy gradient is in fact the driving effect behind electrowetting induced motion. Although few authors report the successful electrowetting-induced transport of proteins and even physiological fluids [14-16], the transport phenomena seem to be affected by the adsorption of the biomolecules. Although electrochemical properties of these samples are suggested to be able to alter the transport of the microdroplets and to affect the value of the saturation angle, due to local modification and/or divergence of the electric fields near the contact line, very little research is yet reported which tries to address these issues. In line with this, the present work aims at characterizing the dynamic behaviour of droplets of biofluids, such as mock blood plasma and BSA protein over enhanced surfaces with and without electrostatic actuation. The best performing enhanced surface is chosen based on the characterization of wettability (static and dynamic contact angles) as well as on the analysis of droplet impact at small velocities. For comparative purposes, one will also analyse the behaviour of droplets of NaCl solutions with different concentrations. Afterwards, the static is characterized under electrostatic actuation. This information is complemented with the dynamic analysis of the contact line motion (inducing droplet spreading) under electrostatic actuation, following the procedure reported in [18].

Varying the pH media for the BSA solutions is also investigated in the present work, as it is expected to alter the charge density inside the bulk of the droplet and affect the electrostatic actuation. Few work has also been performed to investigate this issue, exception made, for instance, to [15], who used a system to study EWOD in solutions of BSA, hen egg white lysozyme and DNA from calf thymus. These authors detected biomolecular adsorption and suggest that it can be prevented or minimized by limiting the applied potential, by selecting the appropriate pH of the solution and the polarity of electrodes. They proposed two mechanisms of biomolecular adsorption under confined conditions EWOD: passive adsorption resulting from hydrophobic interactions and electrostatic adsorption triggered when an external electric field is applied. [17] report a significant dependence on pH, ionic strength, and the polymer composition can influence the behaviour of electrowetting.

Materials and methods

The experimental set-up is mounted on an optical tensiometer (THETA, from Attesion), so that the computer can control all the droplet formation system. For this stage of the research, large droplets with an initial diameter D_0=3.0±0.2mm are used, to assure a good spatial accuracy of the measurements, which is vital for the precise description of the main fundamental quantities that are being investigated. For the electrowetting tests, the droplets are deposited on the enhanced surfaces. In the absence of electrostatic actuation, the spreading is forced through impact over the surfaces with velocities U_0 ranging from 0.44 m/s. As aforementioned in the Introduction, the experiments addressing droplet impact are made to choose the best performing surfaces, i.e. those rendering the most hydrophobic behaviour for all the biofluids used, in both static and dynamic conditions. All the tests are performed inside a Perspex chamber saturated with the working fluid at room temperature. This chamber has four 55x55mm^2 quartz windows to avoid distortion that introduces errors in the image-based techniques. The enhanced surfaces are made from a silicon wafer and are micropatterned using square structural pillars. Numerous surfaces were prepared, whose hydrophobicity was tested based on contact angle measurements performed with water.

At the end, only the surfaces, with the topographical characteristics depicted in Table 1 were used with the biofluids. Here *a* is the side length of the square cross-sectional area of the pillars, h_R is their height and λ is the pitch between them. Additional superhydrophobic surfaces made from aluminum and Teflon are also used.

Table 1: Topographical characteristics of the enhanced surfaces used in the present work.

Surface	Material	Nº	*a* [μm]	h_R [μm]	λ [μm]	R_a [μm]	R_z [μm]
Micro-strutured	Silicon wafer	S1	134	23	171	-	-
	Silicon wafer	S2	173	23.4	112	-	-
Stochastic profiles	Coated Al	S3	-	-	-	4.2	8
	PTFE	S4	-	-	-	~0	~0

Surface topography is characterized using a Dektak 3 profile meter (Veeco) with a vertical resolution of 200Angstroms. For the superhydrophobic aluminum and Teflon (PTFE – polytetrafluoroethylene) surfaces, which depict a stochastic roughness profile, surface topography was quantified by the mean roughness (determined according to standard BS1134) and by the mean peak-to-valley roughness (determined following standard DIN4768), as performed in previous work (e.g. [19-21].) The contact angles were measured at room temperature (ca. 20°C) for all the liquid/surface pairs considered in the present study, using the optical tensiometer THETA (Attension). Five to six consistent measures were taken for each sample using the sessile drop method. Images of the deposited droplet were taken using a monochrome video camera coupled with a microscope. The images size is 640×480pixels and the spatial resolution of the system for the current optical configuration is 15.6μm/pixel. The images were post-processed by a drop detection algorithm based on Young-Laplace equation (One Attension software). The accuracy of this kind of algorithms is argued to be of the order of ± 0.1º (e.g. [22]). Contact angle hysteresis was assessed at room temperature as described by Kietzig [23]. Briefly, a small water drop is dispensed from a needle and brought into contact with the surface. The volume of the drop is increased and the advancing contact angle is taken as the one just before the interface diameter increases. Afterwards, the drop diameter is decreased and the receding contact angle is taken as the one just before the interface diameter decreases [23]. Then, complementary information is given by the spreading diameter, which is obtained from high-speed visualization. The high-speed images were taken at 2200fps using a Phantom v4.2 from Vision Research Inc., with 512x512pixels@2200fps resolution and a maximum frame rate of 90kfps. For the present optical configuration the spatial resolution is 25μm/pixels and the temporal resolution is 0.45ms. The spreading diameter is evaluated based on image post-processing procedures. The spreading diameter measured with and without electrostatic actuation is averaged over 6 events, obtained at similar experimental conditions. Accuracy of the measurements is evaluated to be ±25μm.

Sample preparation

Throughout the study various solutions were used: sodium chloride, blood plasma mock (5.6mM glucose, 100mM NaCl and 1.2mM BSA) and BSA protein. The solutions of NaCl and BSA were tested at different concentrations and were all prepared in distilled water. To study the effect of altering the pH on the protein BSA was necessary to prepare two buffer solutions, one of citrate, to pH=5, and other carbonate to pH=10. The pH measurements were performed in Metrohm 691 pH meter.

Electrowetting configuration

The electrostatic actuation is performed in a single-plate configuration, following the schematics presented in Figure 1.

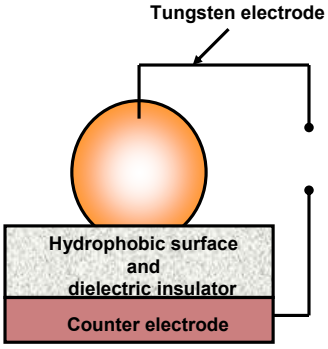

Figure 1. Schematic showing the configuration used for the electrowetting actuation experiments.

A 10μm Teflon film is used as the dielectric. As recommended by Restolho *et al***.** [25] a very thin film of sodium chloride was placed between the counter electrode and the dielectric to avoid the presence of an air gap. The electrode dipped inside the droplet is a tungsten wire with 25μm diameter (Goodfellow Cambridge Ltd). The counter electrode is a copper cylinder. Both electrodes were connected to a Sorensen DCR600-.75B power supply and DC voltage is applied in increments of 25V. Reversibility measurements are performed decreasing the voltage from the maximum value down to 0V, also in steps of 25V. At least 6 tests are performed to obtain an average representative curve (contact angle vs. applied voltage) for each condition tested. An illustrative curve obtained for NaCl (200mM) is depicted in Figure 2.

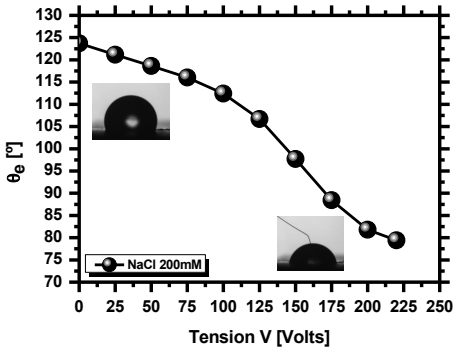

Figure 2: Illustrative curve of the contact angle in function of the applied voltage to a drop of NaCl with a concentration of 200mM. The droplets have an initial diameter D_0=2.8mm.

Viability Tests

After the electrostatic actuation, one must infer if the samples suffered significant modifications and if they are still viable. For the biological fluids used here, a major concern is the stability of the BSA protein, as this may denature due to the electrostatic actuation. This was checked by measuring the absorption spectra of the BSA solutions, before and after the actuation experiments, using a NanoDrop 2000c/2000 UV-Vis spectrophotometer (Thermo Scientific). The scans were performed in the 250-400nm wavelength range using 2µl of solutions.

Results and Discussion

Static and dynamic wetting without electrostatic actuation

Table 2 summarizes the static angles measured for each of the liquid-surface pairs considered here. The results evidence that all the selected surfaces kept hydrophobic angles (over 100º) for all the liquids tested. The experiments performed also show no significant effect of varying the concentrations of NaCl or protein (BSA) in the solutions, so that only the results obtained for one illustrative concentration are depicted here. It is worth mentioning that although the static angles are overall quite high, the hysteresis measured for surfaces S1 and S2 was higher than 30º, which is indicative that large energy dissipation may occur at the contact line during droplet motion. The PTFE surface rendered a hysteresis of 19º and only surface S4 rendered a very low hystreresis, of the order of 8º, for the various liquids tested (i.e. the surface has superhydrophobic properties). This can be a problem during electrostatic actuation, since it may preclude the occurrence of reversibility. To further investigate this issue and before submitting the samples to electrostatic actuation, forced droplet spreading was further characterized, by impacting the droplets on the surfaces at low velocities. The temporal evolution of the resulting spreading diameter is depicted in Figure 3. In order to avoid an exhaustive description, results are only presented here for the spreading of plasma mock over surfaces S1-S4.

Given that the hysteresis is significantly high for surfaces S1 and S2, pinning of the contact line may occur on the micro-patterns. Consequently, energy is dissipated at the contact line, so that a smaller spreading diameter of the droplets is observed over these surfaces. Also, the recoiling is lessened, thus suggesting that one will have an electrowetting induced irreversible motion over these surfaces. This behavior contrasts with that of surface S3, for which the droplet shows evident recoil after spreading, as a result of the low dissipation occurring during droplet motion (low hysteresis). The PTFE surface renders a less evident recoiling phase, when compared to surface S3, but still noticeable. Hence, based on this analysis, only surfaces S3 and S4 (the PTFE surface) were used in the electrowetting tests.

Table 2. Equilibrium contact angles for the representative pairs liquid-surface used in the present work.

	Water	NaCl (100mM)	Plasma mock
S1	140±6°	144±5°	145±5°
S2	116±5°	111±5°	116±6°
S3	152±4°	148±6°	150±6°
PTFE (S4)	112±5°	112±6°	112±5°

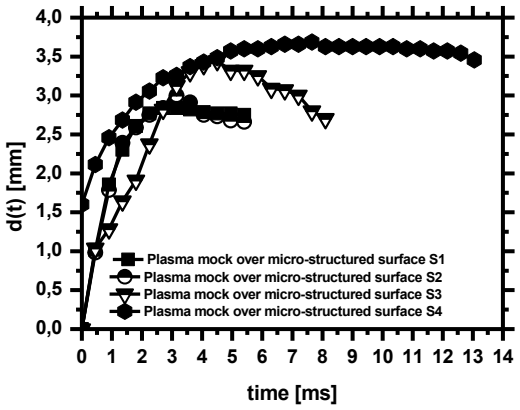

Figure 3. Spreading of a plasma mock droplet D_0=3.2mm, U_0=0.44m/s over various surfaces without electrostatic actuation

Static and dynamic wetting with electrostatic actuation

Droplet spreading induced by electrowetting was investigated by measuring the static and dynamic conditions. For the measurement of the static contact angles, the droplets were deposited on the substrates and actuated with gradually increasing voltage. For illustrative purposes, only the results with the PTFE substrate are shown as the surface is representative in terms of the static wetting effects as aforementioned, but one has not to deal with the additional effect of the regular micropattern, which requires deeper investigation. Also, surface S3 was too thick to allow the tests at this stage of the work. In

line with this, Figure 4 depicts the static contact angle as a function of the applied voltage for NaCl and BSA for different concentrations. The results in the Figure 4 suggest a mild effect of the concentration for the various solutions. Hence, for NaCl, electrowetting is slightly enhanced (i.e. the contact angle decreases more with the applied voltage and this decrease is observed from lower values of the voltage) as the concentration increases from 50mM to 200mM. Then, electrowetting induced decrease of the contact angle becomes again less efficient for concentrations of 400mM. This suggests an optimum concentration around 100mM for the conditions tested here.

Most of the authors (*e.g.* [11,25]) report an insignificant effect of the concentration of NaCl on the electrowetting-induced decrease of the contact angle. However, these authors usually work with smaller droplets and lower salt concentrations. [17] and [7] suggest a possible modification of the electrical fields due to adsorption of the salts by the dielectric substrate which may in turn affect the electrowetting. The contact angle of the BSA solutions seem to be more difficult to decrease at lower actuation voltages, but shows a steeper slope for higher voltages, which suggests that the BSA transport is also promoted by small increases of its concentration. However, a further increase of the concentration of the protein leads to a saturation situation for which the contact angle almost does not change. This may be also explained by the adsorption of the protein by the dielectric substrate, as Teflon (PTFE) has high affinity to biomolecules and proteins, including BSA [27]. Hence, as the adsorption occurs, the contact angle drops to a limit value after which it cannot change. This effect is strongly enhanced by small increases of the concentration of the protein, which promote the adsorption, lowering the contact angle and making the motion of the contact line more difficult for the latest parts of the test, which correspond to the highest actuation voltage. It is worth mentioning that the induced advance of the contact line was observed to be irreversible for all the electrowetting tests performed, probably due to the relatively high hysteresis measured for the Teflon.

Additional information was obtained by observing the transient morphology of the actuated droplets, by high-speed visualization. In this case, a new droplet is used for each droplet, to infer if the motion of the contact line was being influenced by the irreversibility caused by the decrease of the contact angle. Qualitative analysis of the high-speed videos (not shown here) evidences the occurrence of asymmetry in the shape of the droplet due to hysteresis. Also, in some cases the hysteresis leads so significant differences in the motion of the contact line that actually induce the slip of the droplet in the opposite direction. Considering now a more quantitative analysis, Figure 5 shows the temporal evolution of the electrowetting induced spreading of the contact line, for the concentrations reported in Figure 4. The spreading velocity now is much smaller, when compared to that obtained in the spreading induced by droplet impact and in this case the force balance is mainly governed by electrocapillar effects (inertia and viscosity are negligible). Here, t=0 corresponds to the time instant when the droplet is actuated. The curves obtained here are qualitatively in agreement with those reported by [23], exception made to the fact that our curves depict more oscillations.

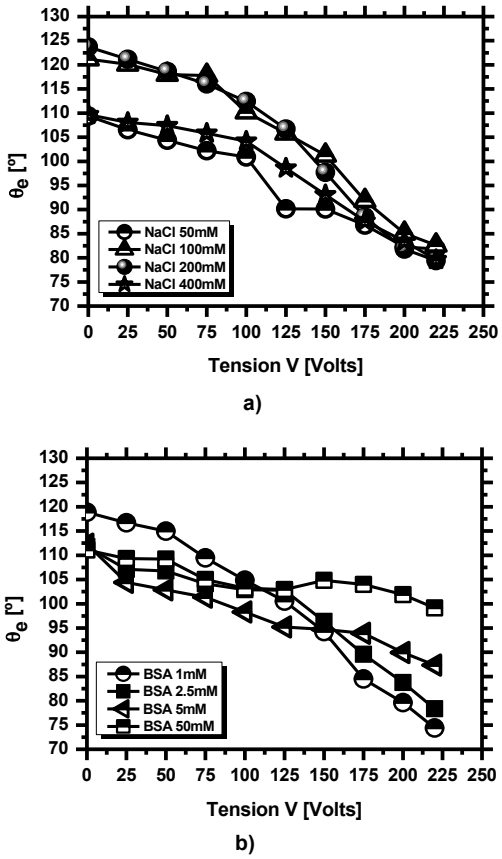

Figure 4. Contact angle as a function of the applied voltage for solutions of **a)** NaCl, **b)** BSA, for different concentration of the solutions. The droplets have an initial diameter D_0=2.8mm

Overall the spreading diameter is in agreement with the trends suggested in Figure 4, given that the electrowetting seems to be slightly promoted by the increase of the concentration. Here, the difficulty in the transport of the protein is not so clear, as the highest concentration BSA solution actually depicts one of the largest spreading diameters for the highest actuation voltage. Hence, the apparent limitation in droplet

motion suggested in the static analysis for the solutions with higher concentration of BSA may be indeed related to local wetting modifications resulting from the long period that is available for adsorption of the molecules by the dielectric substrate.

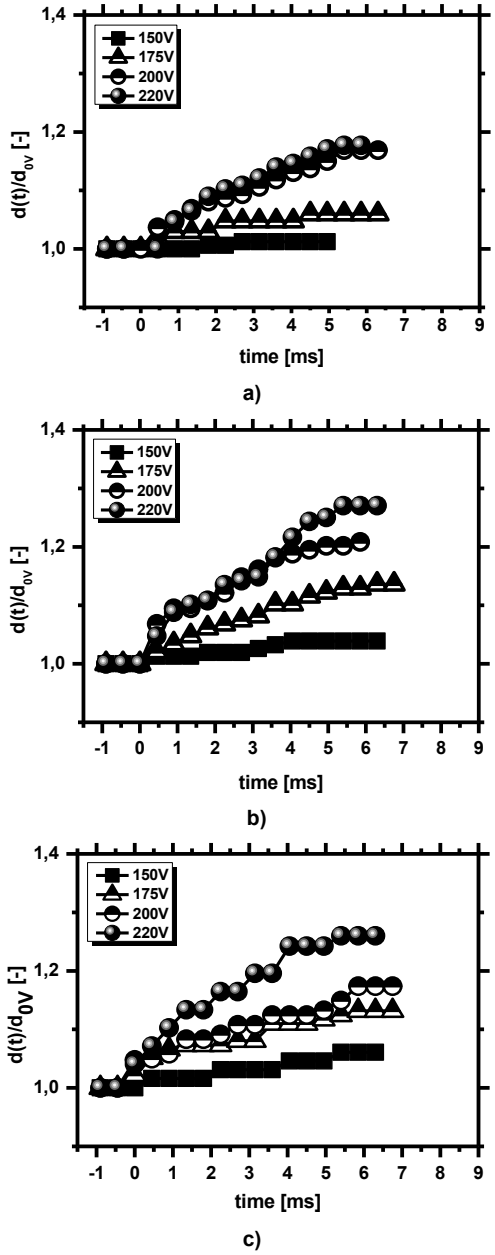

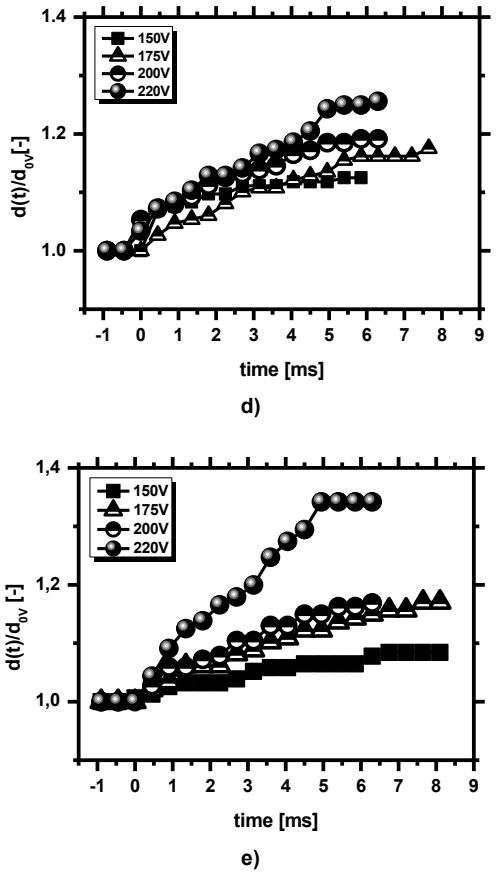

Figure 5: Electrowetting induced spreading of the contact line for solutions of **a)** NaCl (50mM), **b)** NaCl (100mM), **c)** NaCl (200mM), **d)** BSA (1mM) and **e)** BSA (2.5mM). The droplets have an initial diameter D_0=2.8mm.

Effect of pH

The effect of pH was studied only in the BSA solutions because changing the pH of the media to distinct values, far from the isoelectric point of the protein (4.7) [15], may affect the adsorption process but also may promote a modification of the charge density in the bulk liquid of the droplet. Thus, the effect of pH on the evolution of the static angle is not very evident, as seen in Figure 6, but there appears to be a tendency for the angles to become slightly lower, while the pH 5 to 7 is increased and 10. However, for high voltages the contact angle values obtained for pH=5 come to be identical to those obtained for higher pH's, which tend, again to saturate in a constant value.

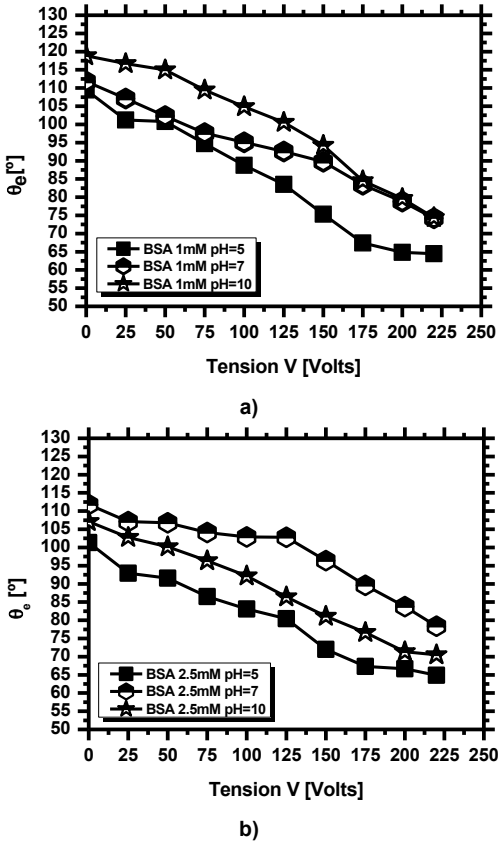

Figure 6: Effect of pH on the evolution of the static contact angle with the applied voltage to BSA solutions at different concentrations. **a)**1mM, **b)**2.5mM. The initial droplet diameter is Do = 2.8mm.

The spreading diameter analysis, depicted in Figures 7 and 8 shows a trend towards higher pH media favoring the spreading of droplets induced BSA to concentrations of 1mM and 2.5mM, respectively. In addition to the effect of adsorption of BSA cited above, which for the long duration tests for static angles measurement promotes saturation at high-tension values, as the contact angle cannot lower anymore, for these dynamic conditions, the adsorption is lessened and, at the beginning, may still allow the spread. In addition, the variation of the pH to higher values may motivate a change in the charge density on the droplet, as suggested by [26], which justifies the higher induced spreading in drops to pH=7 and pH=10.

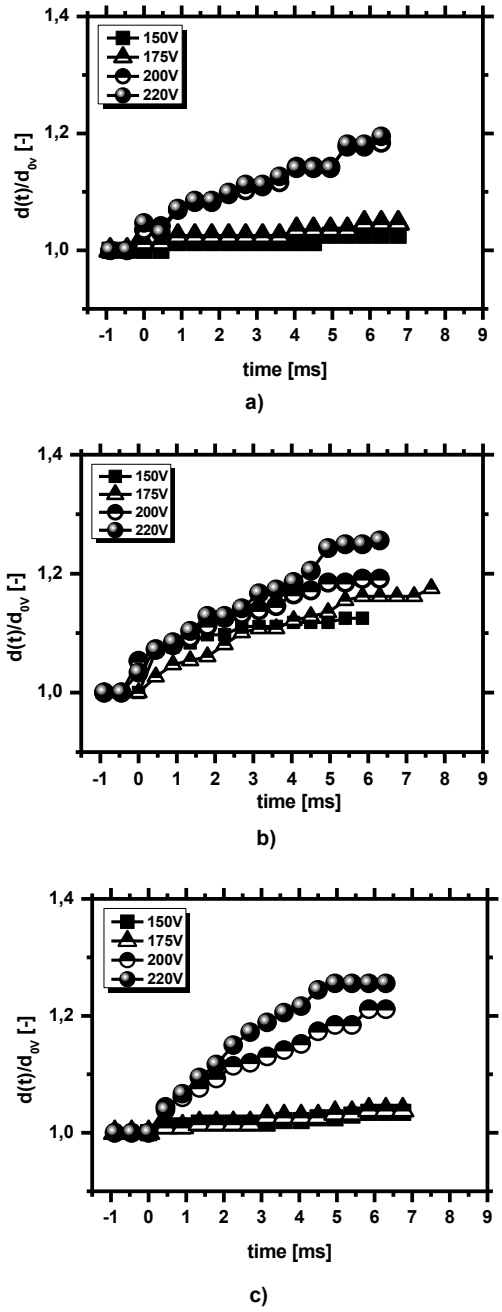

Figure 7: Effect of pH on the spreading diameter induced by electrostatic actuation in 1mM BSA solution: **a)** pH=5, **b)** pH=7, **c)** pH=10. The initial droplet diameter is Do = 2.8mm.

Thus, the basic media (pH=10) the buffer solution used was a carbonate. It is known from the literature adsorption of protons (H+) and hydroxide ions (OH) surfaces to give rise to a surface potential. Accordingly, when the pH is above the isoelectric point of the protein, [26] report that a rearrangement of the chains of BSA with the substrate should occur, which results in an opposed trend to the remaining liquid drop. Thus, if the loads in the droplet are

repulsive, the chains within the substrate become attractive, locally favoring the spreading of the drop. Thus, increasing the pH favors the occurrence of two processes, which in the long term tests are competitors, but in short time intervals favor the spreading of the droplet, while the limiting value of the contact angle is not reached yet.

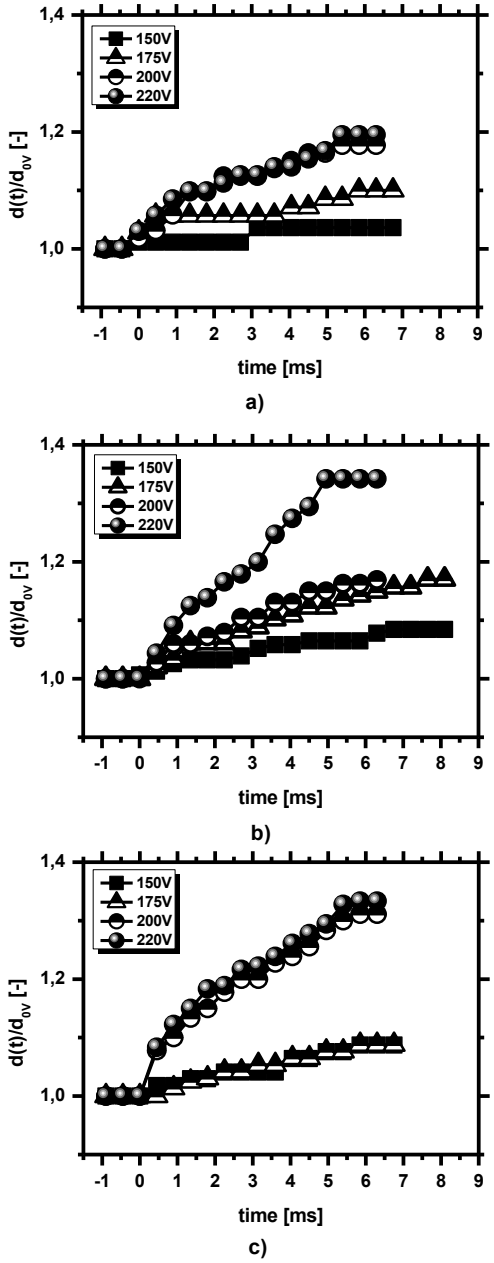

Figure 8: Effect of pH on the spreading diameter induced by electrostatic actuation in 2.5mM BSA solution: **a)** pH=5, **b)** pH=7, **c)** pH=10. The initial droplet diameter is Do = 2.8mm.

Looking at the adsorption mechanisms proposed by (Yoon & Garrell, 2003), the adsorption of the BSA occurs here by a passive mechanism, which is not solved by varying the pH. Actually, the results obtained here suggest that the adsorption is promoted for basic media. This is an issue that requires a deeper investigation on the adsorption mechanisms that are occurring, so that a compatible material can be chosen, which lessens the adsorption, or the transport process will not viable.

Viability of the samples

The impact of electrostatic actuation on the stability of BSA was inferred by comparing the absorption spectra of the solutions, before and after actuation. The tests were performed for the solutions with the lowest and highest concentrations of 1mM and 50mM, respectively. The obtained spectra, shown in Figure 9 reveal that BSA does not suffer any structural modification, as the spectra obtained before and after electrostatic actuation are similar. The increase in the absorption peak observed at 50mM concentration, after electrowetting is ascribed to droplet evaporation, which leads to an increase in the concentration of 1.5 times. This increase in the concentration is estimated to be indicative of a decrease in the volume of the droplet by evaporation of approximately 30%. To assure that droplet evaporation is actually caused by electrowetting and not by mass diffusion to the surrounding air, the absorption spectra were repeated on the samples by simply depositing the droplets over the substrate and waiting the time period that was required to complete tests, with electrostatic actuation.

The results of such tests show no evident modification in the peaks of the spectra, thus corroborating the hypothesis that the evaporation of the droplet is indeed caused by electrowetting. This maybe a problem for applications in lab-on-a-chip devices, particularly for diagnostic purposes that rely on the detection of the protein (or any other component transported in the droplet) and therefore deserves more attention in future studies.

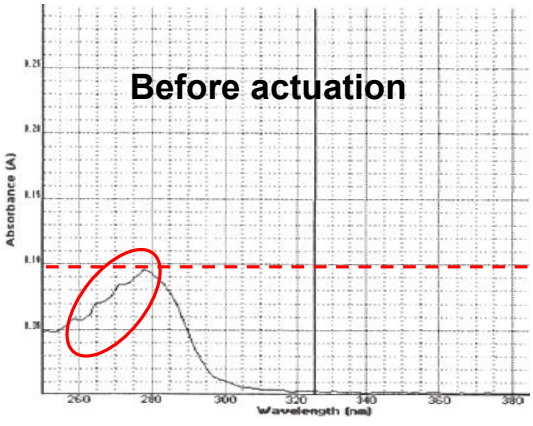

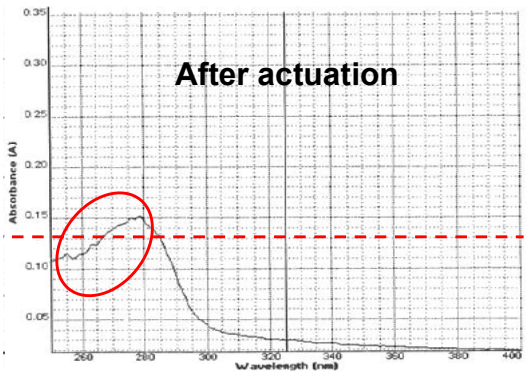

Figure 9. Absorption spectra obtained for the BSA solution with 50mM concentration before and after electrowetting.

Final Remarks

The present paper addresses the forced spreading of droplets of biofluids over enhanced surfaces, with and without electrostatic actuation, in the context of sample handling in lab-on-a-chip applications. The best performing enhanced surfaces are chosen based on the characterization of the wettability, quantified by the static contact angle and by analysing the temporal evolution of the droplet diameter within a spreading motion forced by droplet impact at small velocities. The tests consider the use 2-3μL droplets of NaCl, plasma mock (100mM NaCl, 1.2mM BSA, 5.6mM glucose) and BSA solutions with different concentrations. Droplet spreading induced by electrowetting was investigated for static and dynamic conditions. The results show a mild effect of the concentration of the salt and of the protein BSA in promoting droplet motion by electrowetting. The static analysis of the electrowetting (based on the gradual decrease of the static contact angles for increasing applied voltages equilibrium angles) showed relatively low concentration of the BSA lead to a saturation situation in which the contact angle does not change. This effect is attributed to the passive adsorption of the BSA by the substrate, which is promoted as the concentration of the protein is increased. For the static angle measurements, in which the droplet stays over the substrate for longer periods, this mechanism is more likely to affect the variation of the contact angle, which does not change at the highest actuation voltages.

This information was complemented with the analysis of the spreading diameter induced by the electrostatic actuation. In this case, the time in which the droplet is deposited on the substrate is lower, so the adsorption effect is lessened. Instantaneously, it actually allows the droplet to spread. Hence, the apparent high saturation angles can be indeed attributed to the adsorption of the molecules by the dielectric substrate, which induce modifications of the wettability, if the droplet stays in contact with the dielectric for enough time. Varying the pH media for the BSA solutions was also investigated, as it is expected to alter the charge density inside the bulk of the droplet and affect the electrostatic actuation.

The effect of pH on the static angle is not very evident. The angles seem to be slightly lower, while the pH 5, 7 and 10 is increased, however, due to the adsorption, which is actually promoted by basic media, for high voltages, the contact angle values obtained for pH=5 come to be identical to those obtained for higher pH's, which tend to saturate for a constant value. The spreading diameter shows a trend to increase towards higher pH media, for BSA concentrations of 1mM and 2.5mM, which is attributed to a rearrangement of the chains of BSA with the substrate.

To infer on the viability of the protein, the absorption spectra of the samples before and after electrowetting were analyzed. The results reveal that the samples remain unchanged after electrostatic actuation, but the transported droplet evaporates, causing an increase of the concentration of the biological sample.

Acknowledgements

The author is grateful to Fundação para a Ciência e a Tecnologia (FCT) for partially financing the research under the framework of project PTDC/EME-MFE/109933/2009). The work was also partially financed by FCT through the project RECI/EMS-SIS/0147/2012. Finally the author would like to thank Professor J. L. Mata for his valuable help in setting up the electrowetting configuration.

References

[1] Hong, L. & Pan, T., 2011. Surface microfluidics fabricated by photopatternable superhydrophobic nanocomposite. Microfluidics and Nanofluidics, 10(5), pp.991–997.
[2] Park, J.K., Lee, S.J. & Kang, K.H., 2010. Fast and reliable droplet transport on single-plate electrowetting on dielectrics using nonfloating switching method. Biomicrofluidics, 4(2), pp.1–8.
[3] Jakeway, S.C., de Mello, A.J. & Russell, E.L., 2000. Miniaturized total analysis systems for biological analysis. Journal of Analytical Chemistry, 366(6-7), pp.525–539.
[4] Hong, J.W. & Quake, S.R., 2003. Integrated nanoliter systems. Nature Biotechnology, 21, pp.1179–1183.

[5] Barbulovic-Nad, I. et al., 2008. Digital microfluidics for cell-based assays. Lab on a chip, 8(4), pp.519–526.
[6] Mohamed, H., Turner, J.N. & Caggana, M., 2007. Biochip for separating fetal cells from maternal circulation. Journal of Chromatography A, 1162(2), pp.187–192.
[7] Mugele, F. & Baret, J.-C., 2005. Electrowetting: from basics to applications. Journal of Physics: Condensed Matter, 17(28), pp.R705–R774.
[8] Cooney, C.G. et al., 2006. Electrowetting droplet microfluidics on a single planar surface. Microfluidics and Nanofluidics, 2(5), pp.435–446.
[9] Jones, T.B., 2005. An electromechanical interpretation of electrowetting. Journal of Micromechanics and Microengineering, 15(6), pp.1184–1187.
[10] Pollack, M.G. et al., 2011. Applications of electrowetting-based digital microfluidics in clinical diagnostics. Expert review of molecular diagnostics, 11(4), pp.393–407.
[11] Berge, B., 1993. Electrocapillarity and wetting of insulator films by water. Comptes Rendus De L'Academie Des Sciences, Séries II, 317, pp.157–163.
[12] Kuo, J.S. et al., 2003. Electrowetting-induced droplet movement in an immiscible medium. Langmuir, 19, pp.250–255.
[13] Bahadur, V. and Garimella, S.V., 2006, J. Micromechanics and Microengineeering, 16, pp. 1494-1503.
[14] Srinivasan, V., Pamula, V.K. & Fair, R.B., 2004. An integrated digital microfluidic lab-on-a-chip for clinical diagnostics on human physiological fluids. Lab on a chip, 4, pp.310–315.
[15] Yoon, J.Y. & Garrell, R.L., 2003. Preventing biomolecular adsorption in electrowetting-based biofluidic chips. Analytical Chemistry, 75(19), pp.5097–5102.
[16] Wheeler, A.R. et al., 2004. Electrowetting-Based Microfluidics for Analysis of Peptides and Proteins by Matrix-Assisted Laser Desorption/Ionization Mass Spectrometry. Analytical Chemistry, 76(16), pp.4833–4838.
[17] Quinn, A., Sedev, R. & Ralston, J., 2003. Influence of the Electrical Double Layer in Electrowetting. The Journal of Physical Chemistry B, 107, pp.1163–1169.
[18] Annapragada, S.R. et al., 2011. Dynamics of droplet motion under electrowetting actuation. Langmuir, 27(13), pp.8198–8204.
[19] Moita, A.S. & Moreira, A.L., 2007. Experimental study on fuel drop impacts onto rigid surfaces: Morphological comparisons, disintegration limits and secondary atomization. Proceedings of the Combustion Institute, 31(2), pp.2175–2183..
[20] Moreira, a. L.N., Moita, A.S. & Panão, M.R., 2010. Advances and challenges in explaining fuel spray impingement: How much of single droplet impact research is useful? Progress in Energy and Combustion Science, 36(5), pp.554–580.
[21] Rioboo, R., Tropea, C. & Marengo, M., 2001. Outcomes from a drop impact on solid surfaces. Atomization and Sprays, 11(2), pp.155–165.
[22] Cheng, P. et al., 1990. Automation of axisymmetric drop shape analysis for measurements of interfacial tensions and contact angles. Colloids and Surfaces, 43, pp.151–167.
[23] Kietzig, A.M., 2011. Comments on "an essay on contact angle measurements" - An illustration of the respective influence of droplet deposition and measurement parameters. Plasma Processes and Polymers, 8(11), pp.1003–1009.
[24] Restolho, J., Mata, J.L. & Saramago, B., 2009. Electrowetting of Ionic Liquids: Contact Angle Saturation and Irreversibility. Journal of Physical Chemistry C, 113(21), pp.9321–9327.
[25] Verheijen, H.J.J. & Prins, M.W.J., 1999. Reversible electrowetting and trapping of charge: Model and experiments. Langmuir, 15(20), pp.6616–6620.
[26] Li, Y. et al., 2008. Effects of pH on the interactions and conformation of bovine serum albumin: comparison between chemical force microscopy and small-angle neutron scattering. The Journal of Physical Chemistry B, 112(12), pp.3797–3806.
[27]Rupp, F. & Axmann, D., 2002. Adsorption/desorption phenomena on pure and Teflon® AF-coated titania surfaces studied by dynamic contact angle analysis. Journal of Biomedical Materials Research, 62(4), pp.567–578.